CONCEPTUAL DESIGN OF THE SODIUM-COOLED FAST REACTOR KALIMER-600

DOHEE HAHN*, YEONG-IL KIM, CHAN BOCK LEE, SEONG-O KIM, JAE-HAN LEE, YONG-BUM LEE, BYUNG-HO KIM and HAE-YONG JEONG
Fast Reactor Development Group, Korea Atomic Energy Research Institute
150 Dukjin-dong, Yusung-gu, Daejeon 305-353, Korea
*Corresponding author. E-mail : hahn@kaeri.re.kr

Received May 12, 2007

The Korea Atomic Energy Research Institute has developed an advanced fast reactor concept, KALIMER-600, which satisfies the Generation IV reactor design goals of sustainability, economics, safety, and proliferation resistance. The concept enables an efficient utilization of uranium resources and a reduction of the radioactive waste. The core design has been developed with a strong emphasis on proliferation resistance by adopting a single enrichment fuel without blanket assemblies. In addition, a passive residual heat removal system, shortened intermediate heat-transport system piping and seismic isolation have been realized in the reactor system design as enhancements to its safety and economics. The inherent safety characteristics of the KALIMER-600 design have been confirmed by a safety analysis of its bounding events. Research on important thermal-hydraulic phenomena and sensing technologies were performed to support the design study. The integrity of the reactor head against creep fatigue was confirmed using a CFD method, and a model for density-wave instability in a helical-coiled steam generator was developed. Gas entrainment on an agitating pool surface was investigated and an experimental correlation on a critical entrainment condition was obtained. An experimental study on sodium-water reactions was also performed to validate the developed SELPSTA code, which predicts the data accurately. An acoustic leak detection method utilizing a neural network and signal processing units were developed and applied successfully for the detection of a signal up to a noise level of -20 dB. Waveguide sensor visualization technology is being developed to inspect the reactor internals and fuel subassemblies. These research and developmental efforts contribute significantly to enhance the safety, economics, and efficiency of the KALIMER-600 design concept.

KEYWORDS : SFR, Fast Reactor, Metal Fuel, Sodium

1. INTRODUCTION

The role of nuclear power in electricity generation is expected to become more important in Korea due to the increasing level of demand for electricity and the relatively scarce supply of natural resources in Korea. Since the first commercial nuclear power plant Kori Unit 1 started its operation in 1978, there are now 16 PWRs and 4 PHWRs in operation as of May 2006. According to the "Basic Plan for Long-term Electricity Supply and Demand," eight new nuclear power units will be constructed by 2017. At present, four OPRs are under construction and scheduled for completion between 2010 and 2012: two at the Kori site and two at the Wolsong site. Additionally, four APR1400 plants are scheduled for completion between 2013 and 2016. With these eight additional plants in the nuclear fleet, nuclear power will occupy nearly 33% of the total installed capacity and 47% of the total electricity generation by 2017.

With the operation of nuclear power plants, PWR spent fuel storage spaces at reactor sites are being filled quickly; they are expected to be full by 2016. In 1998, the Korea Atomic Energy Commission decided to construct an away-from-reactor spent fuel storage facility by 2016 for the storage of spent fuels until a policy is established for the spent fuels. R&D on fast reactors and related fuel cycles are now being performed in order to provide the technical basis and support for systems design.

Future nuclear power plants should meet several criteria: effective resource utilization, waste minimization and reduced environmental impacts, economic competitiveness, enhancement of their safety and reliability, proliferation resistance and physical protection.

In order to meet these criteria, the Ministry of Science and Technology established a Comprehensive Nuclear Energy Promotion Plan in 2001 which set out the basic framework of nuclear R&D in Korea. The plan suggests the development of liquid metal reactor technologies for an efficient utilization of uranium resources with an emphasis on the basic key technologies. The scope of the

project under this plan includes reactor design studies, the development of computational tools, and the development of sodium technologies. According to these purposes, the Korea Atomic Energy Research Institute (KAERI) has started to develop sodium-cooled fast reactor (SFR) technologies. In recent years, KAERI has concentrated on the development of the mid-sized SFR KALIMER-600, and its conceptual design was completed in February 2007. This paper focuses on a description of the KALIMER -600 design and the related R&D efforts.

2. GENERAL FEATURES OF KALIMER-600

KALIMER-600 is a fast neutron spectrum reactor that uses liquid sodium as a coolant. It has a capacity of 600MWe. The core generates fission heat of 1523.4MWt and is loaded with metal fuels of U-TRU-Zr. KALIMER-600 is a pool-type reactor and all the primary sodium is contained in a reactor vessel. The pool-type design feature eliminates the possibility of coolant loss by a pipe break and provides a large thermal damping of the system; thus, it yields a slower transient, a longer grace time in the event of an accident, and eventually increases overall plant safety. A schematic configuration of the KALIMER-600 system is shown in Fig. 1.

The safety systems of KALIMER-600 are based on a passive design concept that does not require any active components in case of design basis accidents. KALIMER -600 also has other enhanced safety features such as metal fuels of inherent safety as well as a Self-Actuated Shutdown System (SASS) in the core. From these design features, KALIMER-600 can accommodate unprotected anticipated transients without scram (ATWS) events without the need for operator action and offsite support for three days. Table 1 summarizes the key design parameters of KALIMER-600.

3. DESIGN DESCRIPTION AND RELATED R&D

3.1 Core Neutronics

The core design of KALIMER-600 was developed to increase its proliferation resistance by using a single enrichment fuel without blanket assemblies [1]. The core design targets include a breakeven breeding (or fissile-self-sufficient), a small burnup reactivity swing of less than 1$, and a high discharge burnup greater than 80MWD/kg. The reactor core concept is also characterized by a long cycle length (≥18EFPM), a small sodium void worth (< 8$), and a peak discharge fast neutron fluence of less than 4.0×10^{23} n/cm^2.

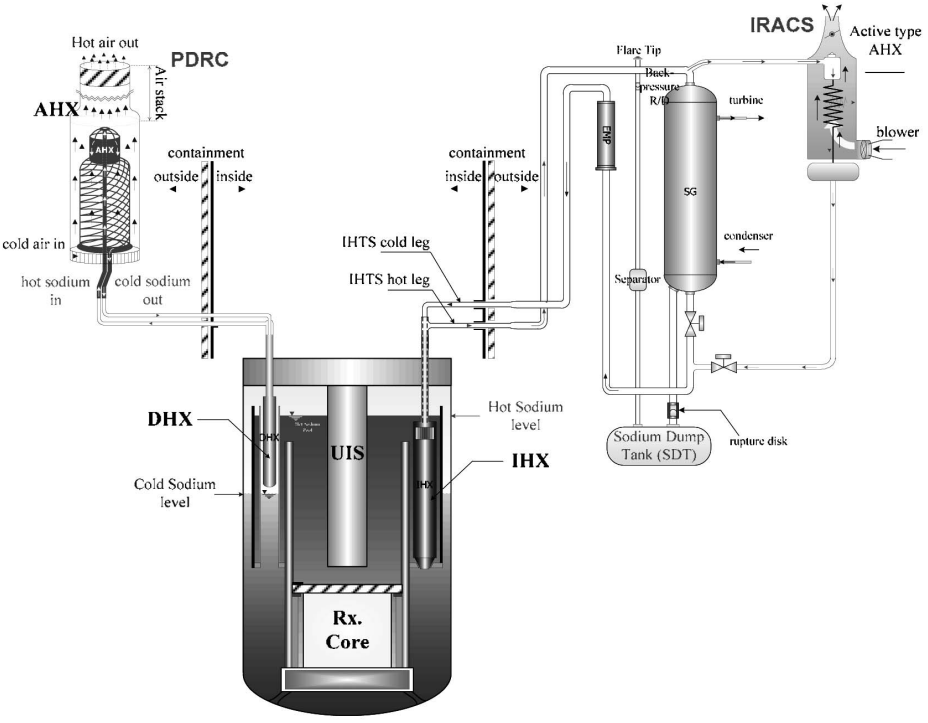

Fig. 1. KALIMER-600 System Configuration

Table 1. KALIMER-600 Key Design Parameters

OVERALL		**PHTS**	
Net plant Power, MWe	600	Reactor Core I/O Temp., °C	390.0 /545.0
Core Power, MWt	1523.4	Total PHTS Flow Rate, kg/s	7731.3
Gross Plant Efficiency, %	41.9	Primary Pump Type	Centrifugal
Net Plant Efficiency, %	39.4	Number of Primary Pumps	2
Reactor Type	Pool Type	**IHTS**	
Number of IHTS Loops	2	IHX I/O temp., °C	320.7/526.0
Safety Decay Heat Removal	PDRC	IHTS Total Flow Rate, kg/s	5800.7
Seismic Design	Seismic Isolation Bearing	IHTS Pump Type	Electromagnetic
CORE		Total Number of IHXs	4
Core Configuration	Radially Homogeneous	**SGS**	
Core Height, mm	940	Steam Flow Rate, kg/s	663.25
Maximum Core Diameter, mm	5209	Steam Temperature., °C	503.1
Metal Alloy Fuel Form	U-TRU-10%Zr	Steam Pressure, MPa	16.5
Cycle Length (EFPM)	18	Number of SGs	2

For the startup core, fresh fuel is composed of recovered LWR transuranics and depleted uranium. In subsequent cycles, a fissile makeup for core loading by recycled TRU is assumed and an equilibrium core is designed such that there is no need for an external feeding of TRUs; hence, only depleted uranium is externally fed. In order to abide by non-proliferation policies, the present breakeven core design employs an integral fuel cycle strategy that uses pyro-processing in which the plutonium and minor actinide nuclides are not separated from each other and the recovery factor of TRU is assumed to be 0.999. In addition, 5% of the rare-earth fission products are assumed recycled, but all other fission products are assumed to be moved to the waste stream.

In a previous design, the single enrichment fuel concept was achieved using special fuel assembly designs in which non-fuel rods (i.e., $ZrH_{1.8}$, B_4C, and dummy rods) were used [2, 3]. In particular, moderator rods ($ZrH_{1.8}$) were used to reduce the sodium void worth and the fuel Doppler coefficient. However, it is now known that this hydride moderator possesses relatively poor irradiation characteristics at high temperatures.

In this work, special fuel assemblies are devised such that the cladding thickness is changed along the core regions for the purpose of power flattening under this single enrichment concept. The cladding thicknesses of the fuel rods in the inner, middle, and outer core regions are 1.02mm, 0.72mm, and 0.59mm, respectively, while the outer diameter of all fuel rods is 9.0mm. A base alloy, which is a ternary (U-TRU-10%Zr) metal fuel, is used for the KALIMER-600 breakeven core.

As shown in Fig. 2, the core adopts a homogeneous configuration in the radial direction that incorporates the annular rings of the inner, middle, and outer fuel assemblies. All the blankets are completely removed in the core to exclude production of weapons-grade plutonium. The core has an active core height of 94.0cm and a radial equivalent diameter (including control rods) of 520.9cm. The core structural material is Mod.HT9. It has low irradiation

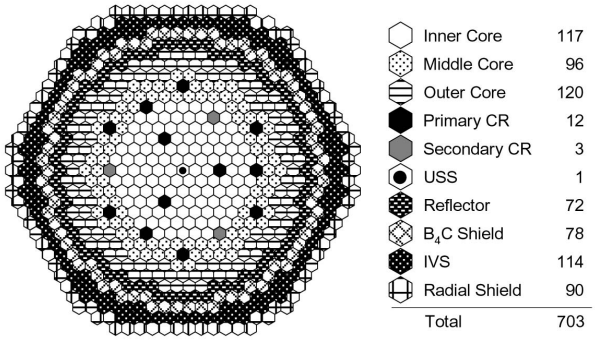

Fig. 2. KALIMER-600 Core Configuration

swelling characteristics, which permits adequate nuclear performance in a physically compact core.

The control rod design satisfies both the one-rod-stuck condition and the unit control-rod worth condition against an unprotected transient over-power (UTOP) event. The ultimate shutdown system (USS), which drops a neutron absorber by gravity, is located in the core center as a means to bring the reactor to a subcritical condition in the event of a complete failure of the normal scram system.

Table 2 summarizes the core design parameters. As described previously, the cladding thickness differs depending on the region. That is, the cladding thickness is decreased from the inner region to the outer region to achieve power flattening without enrichment splitting. However, the smear density and Zr content in the fuel rods are 75% theoretical density (TD) and 10wt%, respectively. As the fuel rod outer diameter is identical for all fuel rods, the volume fraction of the coolant is also identical.

Table 2. Main Core Design Parameters

Parameter	Value
Assembly pitch (cm)	18.71
Duct thickness (mm)	3.7
Fuel rods per assembly	271
Fuel rod outer diameter (mm)	9.0
Cladding Material	Mod.HT9
Cladding thickness (mm)	
IC/MC/OC	1.02/0.72/0.59
Moderator material below fuel	Graphite
Thickness of moderator region (cm)	15.0
Number of control rod assemblies (primary/secondary)	12/3

The core performance results are summarized in Table 3. The average conversion ratio is approximately 1.0 and the fissile Pu gain per cycle is estimated to be 16.9 kg, which satisfies the KALIMER-600 design target of an excess Pu gain close to zero by considering the uncertainties. The cycle length is 18 EFPMs with one-quarter of the fuel being replaced during each refueling time. The burnup reactivity swing is 344 pcm, which is less than 1$. This low burnup reactivity loss leads to reduced control system manipulations as well as to a decrease in the reactivity available for a potential control rod-withdrawal accident. The sodium void worths for a voiding of the flowing sodium coolants both in the active core and the coolant channel of the upper gas plenum are 2583 pcm at BOEC and 2643 pcm at EOEC, which correspond to 7.4$ and 7.6$, respectively. The sodium void worths increase in their magnitude with a burnup due to fission product buildup and Pu quality deterioration.

Table 3. Summary of the Core Performance Results

Parameter	Value
Average conversion ratio	1.0
Cycle length (EFPM)	18
Burnup reactivity swing (pcm)	344
Number of batches	
Inner/Middle/Outer cores	4/4/4
TRU wt% in fuel at BOEC	15.5
Average/peak fuel discharge burnup (MWD/kg)	80.4/125.4
Average power density (BOEC, W/cc)	148.5
Average linear power for fuel (W/cm)	168.3
Power peaking factors for fuel (BOEC/EOEC)	1.498/1.489
Peak discharge fast neutron fluence(10^{23}n/cm^2)	3.98
Sodium void worth (BOEC/EOEC, $)	7.4/7.6
Effective delayed neutron fraction	
BOEC	0.00351
EOEC	0.00348

3.2 Fuel Performance

To maintain the fuel integrity during irradiation, it is necessary to satisfy the fuel design criteria of 1) no melting of the fuel, 2) prevention of eutectic melting at the interface of the fuel and the cladding, 3) limit the cladding strain and cumulative damage fraction to prevent cladding mechanical failure.

Fig. 3 shows the radial temperature distribution of the fuel pin. The centerline peak temperature was much less than the fuel solidus temperature, 1000°C; therefore, there is a sufficient margin to fuel melting. The migration of zirconium in fuel occurs due to a variation of the zirconium solubility in the fuel matrix with the temperature during an irradiation. The concentration of zirconium increases at the center of the fuel. As the fuel solidus temperature increase with the zirconium fraction, there is more margin to fuel melting due to zirconium migration. In the intermediate region of the fuel slug, the zirconium fraction decreases; therefore, the fuel solidus temperature is lowered. However, the fuel melting does not occur as the fuel temperature in that region is low.

Fig. 4 shows the variation of the fuel centerline

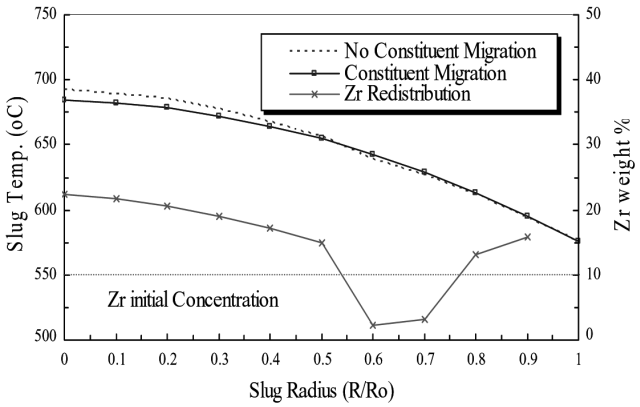

Fig. 3. Radial Temperature Distribution of the Metal Fuel Slug

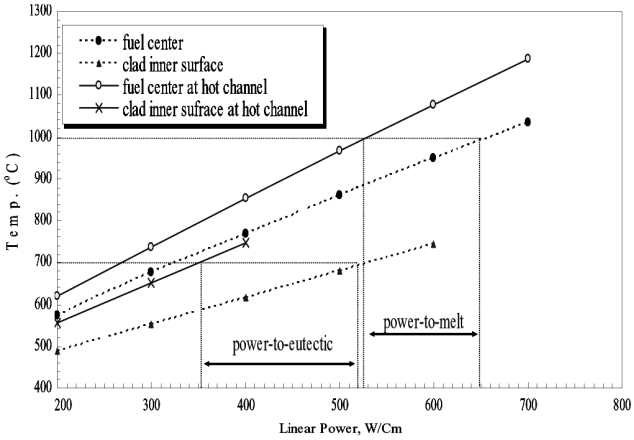

Fig. 4. Variation of the Fuel Centerline Temperature with Linear Power in KALIMER

temperature depending upon the linear heat generation rate of the metal fuel pin. Uncertainties in the coolant flow rate and the fuel local power were conservatively considered in the hot channel case. This shows that the metal fuel in KALIMER has a sufficient margin to the melting temperature. The maximum allowable power to prevent eutectic melting, which occurs at temperatures near 700°C, is approximately 350 W/cm. Therefore, the introduction of a barrier that prevents diffusion of the fuel elements and subsequently eliminates the possibility of eutectic melting will increase the maximum allowable power to greater than 520 W/cm.

As for the cladding mechanical limits, two specific design limits are used. The first is the cladding strain limit, and the second is the cumulative damage fraction (CDF) limit.

The thermal creep strain of the Mod.HT9 cladding is less than the design limit, 1% up to a fuel burnup of 15 at.%. Mod.HT9 cladding has a high thermal creep resistance to satisfy the cladding creep limit up to the fuel discharge burnup. However, there is scant information regarding the material properties for Mod.HT9 cladding. Therefore, irradiation tests of the Mod.HT9 cladding to investigate its irradiation creep and swelling behavior are necessary.

The cumulative damage fraction for Mod.HT9 cladding was analyzed with the effect of a Zr liner barrier. Fig. 5 shows that the minimum cladding thickness to satisfy the CDF limit, 0.001 is 0.63 mm in the case of Mod.HT9 without a Zr liner. For Mod.HT9 with a Zr liner, the minimum cladding thickness was derived as 0.55 mm with a Zr liner of 0.1 mm.

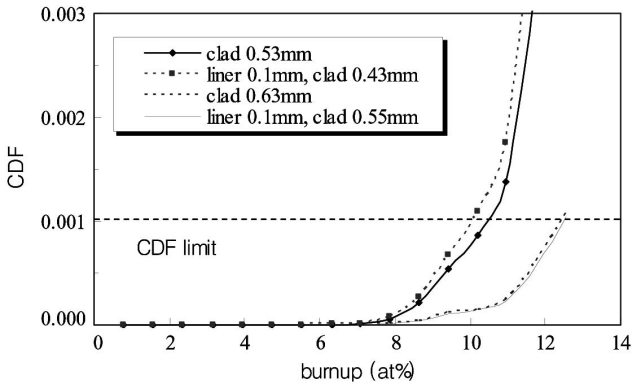

Fig. 5. Cumulative Damage Fraction (CDF) of Mod.HT9 Cladding with the Burnup Values

3.3 System Design Studies

The fluid system of KALIMER-600 is composed of the three major heat-transport systems of the PHTS (Primary Heat Transport System), the IHTS (Intermediate Heat Transport System) and the SGS (Steam Generation System). During normal operations, core heat is transferred to steam generators through the IHTS to produce high-pressure and high-temperature steam.

The primary sodium of KALIMER-600 is contained in a reactor vessel, which eliminates the possibility of primary coolant loss by a pipe break. This provides a large thermal damping of the system, thus yielding a slower transient and longer grace time in the case of an accident. It also increases the overall safety of the plant. IHTS and SGS consist of two identical loops that enhance the flexibility of the plant operation and increase the reliability of the normal heat removal path.

The plant heat balance, shown in Fig. 6, is setup for a 100% rated power condition considering the structure temperature, general characteristics of the BOP and the system economics. The net plant efficiency amounts to 39.4%.

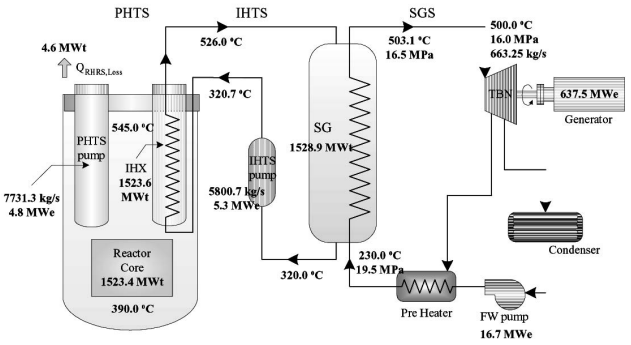

Fig. 6. KALIMER-600 Steady-State Heat Balance

The decay heat-removal system in KALIMER-600 is comprised of a three-layer system that incorporates the safety-grade Passive Decay Heat Removal Circuit (PDRC) and the non-safety-grade active systems of SGS and IRACS (Intermediate Reactor Auxiliary Cooling System).

For a scheduled shutdown, SGS is used from a normal operating condition to a cold shutdown condition; however, in the case of a design-basis accident, the safety-grade PDRC is actuated automatically without operator action or active components. The IRACS is used to support the SGS during the maintenance of the SGS.

The safety-grade PDRC system comprises two independent intermediate sodium loops. Each loop is equipped with a single sodium-sodium decay heat exchanger (DHX), a single sodium-air heat exchanger (AHX), the sodium pipes connecting the DHX with the AHX, and related instrumentation.

When the primary pump shuts down following a reactor trip, as depicted in Fig. 7, the cold pool level rises up to the hot pool level. The primary sodium is then expanded due to the accumulation of the core decay heat. The expanded sodium consequently overflows into the cold pool through the shell-side DHX.

The post-shutdown DHR performance should be assured with a very high reliability in a nuclear reactor system. Therefore, a transient simulation method for the PDRC system was developed and quantitative transient analysis results related to this were obtained using the computer code POSPA [4].

POSPA is a one-dimensional lumped parameter system analysis code for modeling all the naturally circulated thermal portions of the PHTS sodium paths composing the core, the hot pool, DHX shell side, cold pool, and the intermediate loop sodium path including the DHX tube side, the hot leg, the AHX tube side, cold leg, and the AHX shell-side air path including the long air chimney.

Given that the heat transport paths in the PDRC system are strongly coupled with each other, an iterative numerical scheme to simulate the system behavior is required by considering successive time marching. A conversion of the governing equations into finite difference equations was properly made using the upwind-difference scheme with a node system located at the center of the control volume. The fine mesh approach with a larger number of nodes was also used to obtain reasonable calculation results for the given conditions. The fully implicit scheme was employed for a transient term.

Using the developed code, a performance analysis of the PDRC system was carried out for a postulated design basis accident involving the loss of the heat sink due to a station blackout. Fig. 8 shows the transient behavior of the system temperature variations during the postulated condition. As depicted in the figure, the core exit temperature reaches a peak of 651°C just after a reactor shutdown and then decreases. This is mainly due to a discrepancy between the core power decrease and the primary mass flow decrease, but the initial peak value satisfies the design limit of 700°C. The temperature variations of the hot and cold pool show a relatively mild trend with peak values of 557.8°C and 473.5°C, respectively. This shows that the heat removal capacity of the provided PDRC system is sufficient for the postulated design-basis accident condition.

In order to maintain the integrity of the sealing material and to prevent creep fatigue in the reactor head, the reactor head must be cooled during a reactor operation to a maximum temperature of 150°C. For an evaluation of the cooling requirements of the reactor head, steady state, three-dimensional heat transfer analyses were performed using a CFD method.

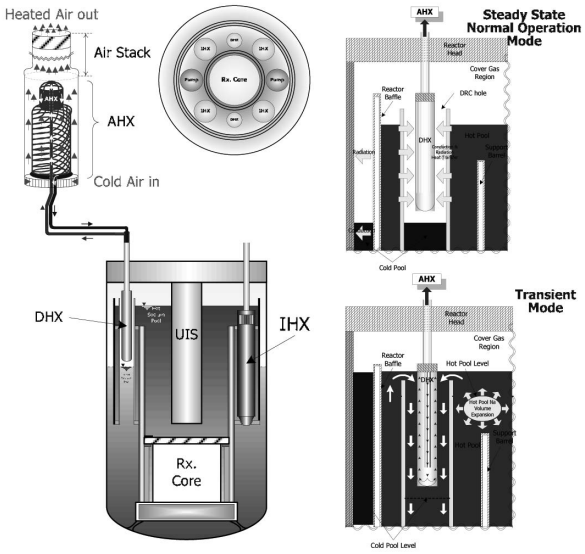

Fig. 7. Configuration and DHR Process of PDRC

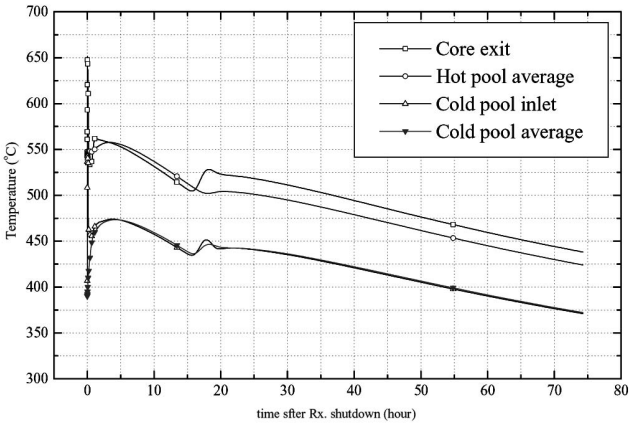

Fig.8. Transient Behavior of the PDRC System

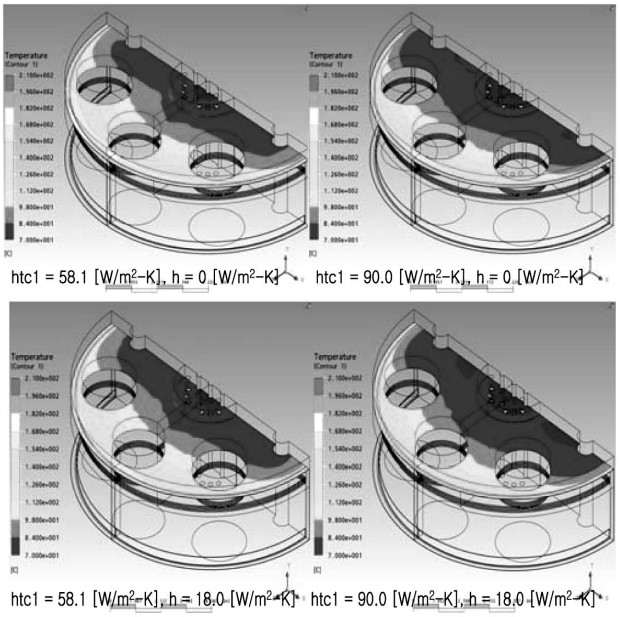

Fig. 9. Temperature Distributions on Bottom of Reactor Head

predicts six instances of the operating temperature on the primary and secondary sides. The sizes of the three regions and the secondary side pressure drop according to the flow rate and the temperature variation in the vertical direction are also predicted well. The temporal variations of the inlet flow rate according to the throttling coefficient, the boiling and superheating boundaries and the pressure drop in the two-phase and superheating regions are obtained from the unsteady analysis. A method for the analysis of the parallel-flow two-phase instability was also proposed, and the method was applied to the analysis of a parallel flow instability experiment conducted at TIT (Tokyo Institute of Technology). The results show that the present method predicts accurate solutions when compared with previous work. The present investigation also shows that it is necessary to investigate parallel flow two-phase instability only when two channels exist, as shown in Figs.10 and 11.

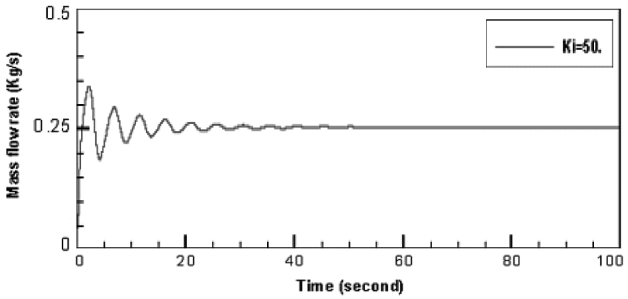

Fig. 10. Variation of the Inlet Mass Flow Rate by Density Wave in Stability (Throttling Coefficient = 50)

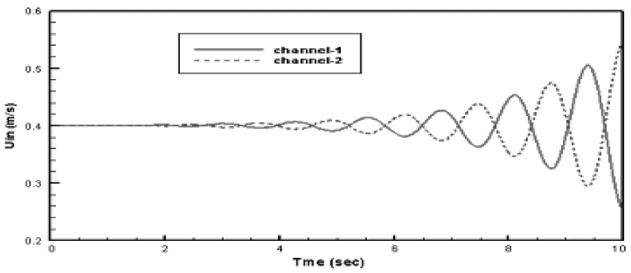

Fig. 11. Time Transients of the Inlet Velocity of the Parallel Flow Instability

For an evaluation of non-linear density-wave instability in a sodium-cooled helically-coiled steam generator, a model was formulated with three regions with moving boundaries. The homogeneous equilibrium flow model was used for the two-phase region and shell-side energy conservation was considered for the heat flux variation in each region. The proposed model was applied to the analysis of the two-phase instability in the JAEA (Japan Atomic Energy Agency) 50MWt No. 2 steam generator. The steady state results show that the proposed model accurately

3.4 Experimental Studies

A number of experimental studies for the verification of the computer model required in the conceptual design of KALIMER-600, in addition to an experimental analysis of the sodium-water reaction phenomena and the acoustic leak detection were performed.

When a significant amount of gas is entrained by sodium

fluctuation, the entrained gas causes a change in the reactivity and reduces the heat removal capability of the coolant in the core [5-9]. An experimental study was carried out to measure the critical conditions for the inception of an air entrainment by breaking the surface wave at the free surface in the water test apparatus. The experiment was performed by changing the diameter of the test section, the inlet nozzle, the average water-level, and the flow rate. Four outlet nozzles were located at a 0.74m elevation from the bottom at a 90 degree angle. The diameters of the nozzles were 0.046m in all cases. The overall range of the flow rate was $1x10^{-3}$~$15x10^{-3}m^3$/sec in the experiment. In this experiment, a bubble could be observed in the test section with the naked eye, and the criterion for the onset of the gas entrainment was set when one or two bubbles appeared and disappeared in the test section.

An experimental correlation that describes the air entrainment condition was developed, as shown in Fig. 12. In this experiment, two cases of air entrainment were observed. The first case is that in which the air entrainment occurred due to the destruction of the surface wave from the center, and the second case is due to a crash of a water wave against the vessel wall. The correlation is described by the ratio between the diameter and height of the vessel, the ratio between the diameter of the nozzle and the height of the vessel, the modified Froude number, and the modified Weber number, as follows:

$$(W_e^*)^{-1/8}\ (\frac{D}{H}) \le\ 0.6209 + 0.113 \ln\left(F_r^*\ \frac{D}{H}\right), \qquad (1)$$

where

$$W_e^* = \frac{\rho g D}{\sigma / D}\ , \qquad (2)$$

$$F_r^* = \frac{d_n}{H}\frac{V}{\sqrt{gH}}\ . \qquad (3)$$

In the above equations, D indicates the diameter of the test section, d_n the diameter of the inlet nozzle, and H the average water-level. Furthermore, V is the average velocity at the nozzle, ρ the density of the water, and σ the surface tension coefficient.

In order to investigate the later phase of a large leak sodium-water reaction event in KALIMER-600, the SELPSTA (Sodium-water reaction Event Later Phase System Transient Analyzer) code was developed. An experimental study was carried out for the verification of the numerical model applied to the code.

The experiment was performed to simulate the long-term system transient responses of a large leak sodium-water reaction event due to a three-double-ended guillotine break of a tube in a 1/10 scale-down mock-up test facility with sufficient considerations of the quasi-steady state features of the SWR event. A total of 83 experimental data sets were obtained for the various test conditions.

A comparison of the SELPSTA results with the experimental data shows fairly good agreement for the pressure transient in the cover gas region, as shown in Fig. 13. For the pressure transients, it was observed that the circulating water flow rate and a flow obstacle had some effect. However, the effect of the air injection position was negligible.

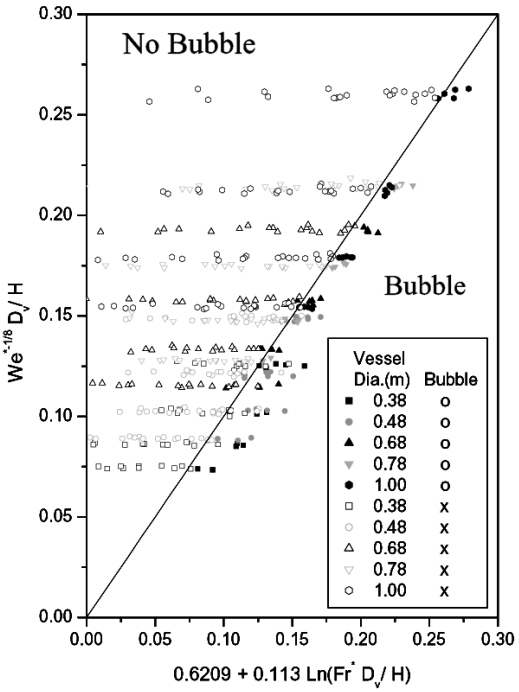

Fig. 12. Critical Gas Entrainment Condition by a Surface Wave at the Free Surface

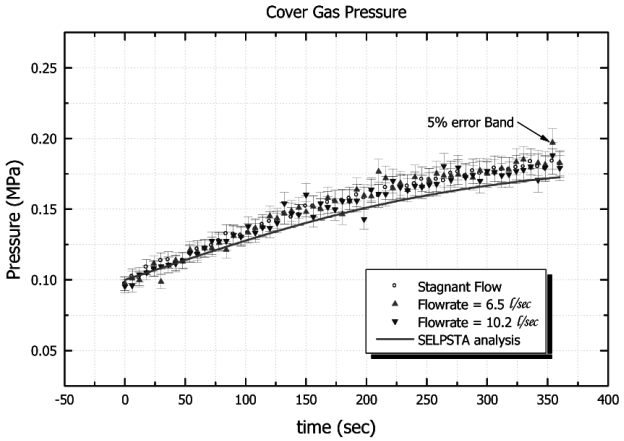

Fig. 13. Comparison of SELPSTA Predictions with the Experimental Data

The trends of the cover gas temperature variation with respect to the test conditions were relatively different compared to the pressure variance. In addition, the water mock-up test had some difficulties with the simulation of the energy transfer between the hydrogen bubbles and the circulating sodium.

The self-wastage phenomena caused by small water/steam leaks were analyzed to evaluate the design criteria and design analysis procedures for steam generators from the point of view of sodium-water reactions. A series of tests was carried out to investigate the enlargement rate of a nozzle hole itself with time for 2.25Cr-1Mo and Mod.9Cr-1Mo steels, which are LMR SG heat-transfer tube materials. The initial size of the nozzle hole in the tests was 0.2mm in diameter, and the initial leak rate of H_2O was 0.38g/sec. The enlargement rate of the nozzle hole was measured at 30 second intervals.

As shown in Fig. 14, the phenomenon during which the size of the nozzle hole enlarged with an increased duration of the steam injection appeared together for the two types of material. The enlargement rate was slightly larger in the 2.25Cr-1Mo steel than in the M.9Cr-1Mo steel. Based on the cross-sectional area of a nozzle hole after 90 seconds of injection testing, it is estimated that the size of the nozzle hole increased by nearly 1.34 times the initial value for the 2.25Cr-1Mo steel.

The detection of a possible leak of steam/water from a tube to the sodium in the SG shell was made via hydrogen concentration measurements, acoustic detection, and/or a measurement of the pressure at a rupture disk piping.

Acoustic leak-detection methodology consists of the neural network and the preprocessing unit of the signals. The preprocessing unit is also used for the 1/n octave-band analysis function, and the selected frequency band is the region of bubbling. After its preprocessing, it is calculated again for the input data of the feature vector for the learning and testing of the neural network, and optimized after tested once again by learning the weight values of the neural network. The raw leak signals are monitored using the optimized neural network to detect a leak state or non-leak state based on the threshold condition that defines the leak.

The performance of the developed acoustic leak detection methodology, which uses sodium-water reaction noises controlled with the attenuation of the KAERI sodium-water reaction signal against the background noise of the PFR S/H (super-heater), was shown to detect a leak up to -20dB according to the learning conditions of the neural network, as shown in Fig. 15.

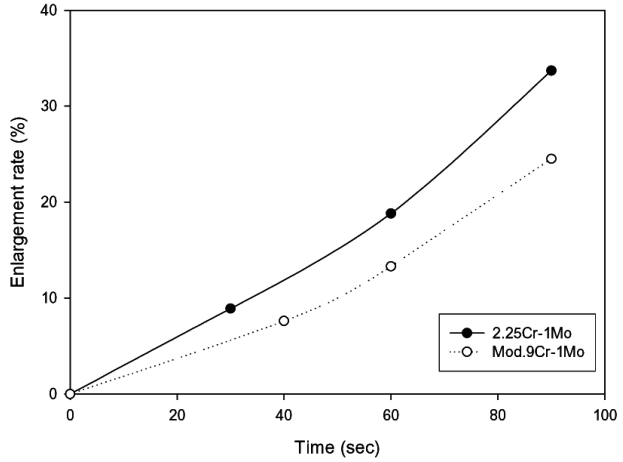

Fig. 14. Enlargement Rate of the Nozzle Hole

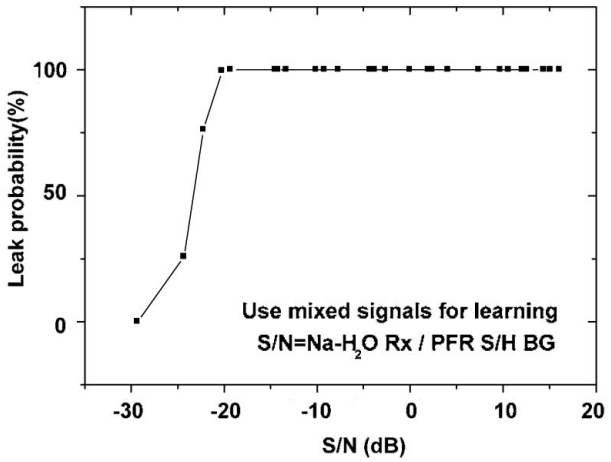

Fig. 15. Leak Probability Tested by the Developed Acoustic Leak Detection Tool.

3.5 Mechanical Structure

The main features of the mechanical structure design of KALIMER-600 are the seismically isolated reactor building, the reduced total pipe length of the IHTS, the simplified reactor core support, and the compact reactor internal structures.

The reactor vessel, which is made of 316-stainless steel, has overall dimensions as follows: 18m in height, 0.05m in thickness and an outer diameter of 11.41m. The total reactor weight is nearly 2,800 tons. Seismic isolation between the ground and lower base-mat in the KALIMER-600 reactor building (W49m x D36m x H54m) is accomplished by 164 seismic isolators that are 1.2m in diameter.

The containment provides a low leakage, pressure-retaining boundary that surrounds the primary system boundary. The containment includes a lower containment vessel to contain reactor vessel leaks and an upper containment structure with a liner which mitigates releases due to postulated severe events. The

containment vessel, which is made of 2.25Cr-1Mo, is 18.25m in height, 0.025m in thickness, and has an outer diameter of 11.76m in the conceptual design. The containment vessel is slightly larger than reactor vessel, and it encloses the reactor vessel. A 15-cm gap between the containment vessel and the reactor vessel contains Argon gas, and the instrument to detect sodium leakage from the reactor vessel is installed in this gap region. This provides a guard vessel for the primary sodium and cover gas if the reactor vessel leaks.

The reactor support structure supports the reactor structures including the reactor vessel, containment vessel, reactor head, reactor internal structures, reactor core, primary sodium, primary pumps, IHXs, in-vessel transfer machine (IVTM), rotating plug, and the instruments. The reactor head, with a diameter of 1176cm and thickness of 50cm, is extended by 30cm in the radial direction, and the extended part of the reactor head forms a part of the reactor support structure. The reactor support structure rests on the head-access area (HAA) floor, and a self-lubricating bearing is installed between the outer part of the reactor head (the reactor support ring) and the HAA floor to allow for radial direction reactor thermal movements by a sliding motion. The reactor support ring is anchored to the HAA floor to restrain vertical movement by bolting, and a lateral seismic restraint is provided by a close fit of the support ring bolts within the radially slotted holes in the support ring.

The reactor head in KALIMER-600 is the top closure of both the reactor vessel and containment vessel. It provides mechanical supports for all PHTS components, including the IHX, primary pump, rotatable plug, reactor internals and primary sodium. The reactor head plate is 50cm thick. It is designed to operate at temperatures lower than 150°C. A low temperature is attained by the inclusion of five horizontal layers of stainless steel insulation and shield plates in the design, the top one of which is installed 45cm below the bottom of the reactor head. The insulation and shield plates are 3cm thick each and are spaced at 2.5cm.

The KALIMER-600 reactor internal structures are composed of the Core Support Structure, the Inlet Plenum, the Support Barrel, the Reactor Baffle, and the Reactor Baffle Plate. The three main functions of the reactor internal structures are as the core support, primary coolant flow path, and component support. The core support structure is a simple detached skirt-type structure, as shown in Fig. 16. The main function of this structure is to support the core assemblies and the fixed internal structures. This provides a very simple core support design, fabrication, and in-service inspection (ISI). The core support structure is fabricated in a forging process, and the number of weld parts is minimized.

The upper internals structure (UIS) is attached to a rotatable plug installed on the reactor closure of the reactor head and cantilevered downward into the reactor hot pool. The total length of the UIS is 10.2m, and the bottom end of a shroud tube is located 5.0cm above the top of the core assemblies during a power operation. The principal functions satisfied by the UIS are the lateral support of the control rod drivelines, the protection of the drivelines from sodium flow-induced vibration, and the support of the above core instrumentation drywells.

The reactor refueling system provides a means of transporting, storing and handling the reactor core assemblies including the fuel, blanket, control, and shield. The system consists primarily of the in-vessel transfer machine, two rotatable plug drives, and the fuel transfer port.

The IHTS piping system in KALIMER-600 connects the IHX, steam generator and secondary electo-magnetic pump (EMP). The piping material is Mod.9Cr-1Mo, which is noted for low thermal expansion and high strength. The shortening of the IHTS piping is a key issue in an SFR design to reduce the construction and maintenance costs. The piping layout was simplified through several optimization studies to obtain the minimum total pipe length while maintaining structural integrity. The hot leg in the IHTS piping has an outer diameter of 60cm and a thickness of 0.95cm, while the cold leg has an outer diameter of 82cm and a thickness of 1.25cm. The total length of the IHTS piping per loop was reduced to 102.6m. Rigid supports, constant spring hangers and snubbers are used for the pipe supports.

There are several R&D items to be implemented in the KALIMER-600 mechanical structure design related to the IHTS piping layout design, the ISI technology development of the reactor internals, the high temperature LBB approach, and the development of structural integrity assessment technology for elevated temperature structures.

The in-service inspection (ISI) and maintenance methods of the reactor system were designed based on the safety goals and on high plant availability. Section XI, Division 3, of the ASME Boiler and Pressure Vessel Code [10] specifies the general type and extent of the ISI required for Class 1, 2 and 3 systems of a liquid metal-cooled plant. Major structures of the reactor system are designed for a low-maintenance operation for the life time of the plant. For equipment or components that directly affect its safety and availability, the system has been provided with features that allow for the removal and in-place maintenance of these components.

Waveguide sensor visualization technology has been developed to inspect the reactor internals using several specific waveguides installed in the hot sodium, as shown in Fig. 16. A waveguide sensor consists of a long strip plate, a wedge and ultrasonic sensors. The sensor can be applicable to under-sodium visualizations, ranging and dimensional gauging. The sensors are installed in the rotating plug on the reactor head. Visualization imaging can be achieved by a scanning of the waveguide sensor assembly above the top plane of the core by the rotation of the rotating plug. A visualization image of the reactor core provides distortion information of the fuel assembly due to neutron-induced swelling. The position of the core structures and components

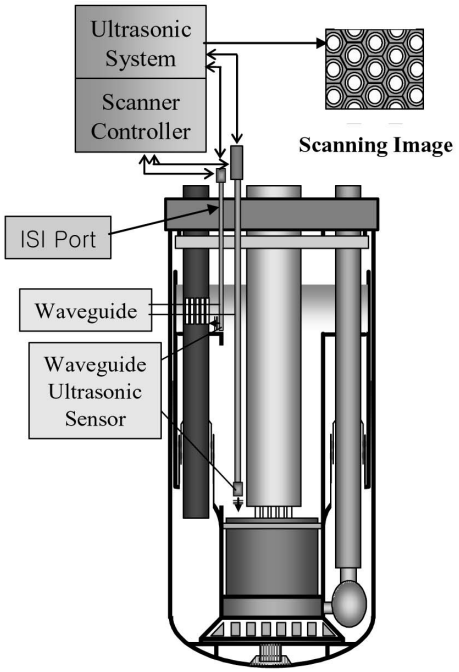

Fig. 16. Visual Inspection Concept Using the Ultrasonic Waveguide Sensor

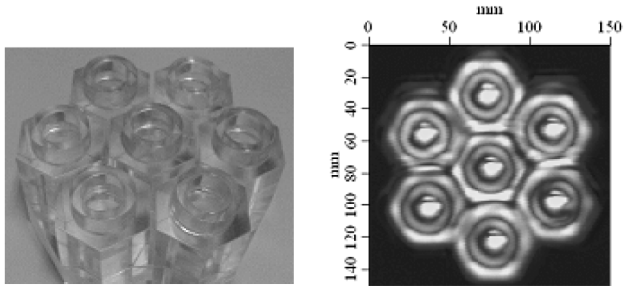

(a) Mock-Up (b) C-Scan Result

Fig. 17. Visualization Image of the Reactor Core Mock-Up Using the Waveguide Sensor

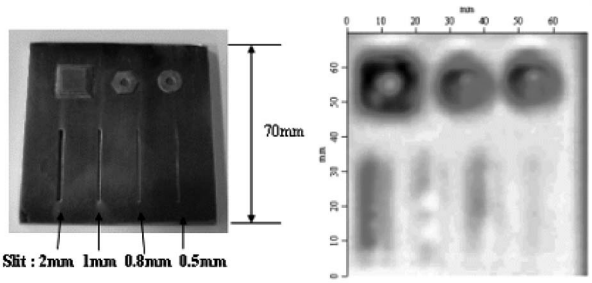

(a) Target Specimen (b) C-Scan Result

Fig. 18. Visualization Image of the Test Target with Slits of Different Sizes and with Loose Parts

can be determined directly through ultrasonic under-sodium visualization before a refueling operation.

To validate the visualization techniques for an underwater condition, a waveguide specimen was fabricated. It consisted of a 250 mm long stainless steel plate that was 15mm wide and 1 mm thick. A C-scan visualization experiment on a shape similar to the reactor core was performed. The visualization image was clearly identified, as shown in Fig. 17. As a second verification, a test target was made of stainless steel with slits of different widths (2mm, 1mm, 0.8mm and 0.5mm) and loose parts (a stepped plate, a small nut and a washer) on the surface. The Fig. 18 shows the visualization image of the test target. The loose part reflections were clearly identified and the slit with a 2mm width was observed successfully.

3.6 Safety Analysis

KALIMER-600 was designed to satisfy the defense-in-depth safety principle and safety design objectives that were established to implement this safety principle in the design. Highly reliable diversified shutdown mechanisms are equipped for a reactivity-control function during an accident or abnormal transients in KALIMER-600.

The reactivity is also controlled by the inherent reactivity feedback mechanisms incorporated in the design. In addition, a uniquely designed passive decay heat-removal circuit provides a heat-removal function. Due to these passive and inherent safety characteristics, the safety of KALIMER -600 is much improved; thus, a benign performance is assured during a selected set of ATWS events without any reactor control and protection system intervention. These events are not HCDA themselves but are designated as bounding events included in the design process to assure public safety, as they have the potential to lead to a large radiological release, a core melt event, or a reactivity excursion.

Preliminary safety analyses were performed to evaluate the plant response, the performance of the inherent safety features, and the margin to the plant safety limits. In the analyses, the system-wide transient and safety analysis code SSC-K [11, 12] was used. The events analyzed are an unprotected transient over power (UTOP), an unprotected loss of flow (ULOF), and an unprotected loss of heat sink (ULOHS). The SSC-K code was the main analysis tool for the system transient analysis during the process of the conceptual design of KALIMER. The code is based on SSC-L, originally developed at BNL to analyze loop-type LMR transients [13]. The SSC-K code aims at handling a wide range of transients, including normal operational transients and anticipated unprotected events in a pool-type reactor. Therefore, both a model development and its verification were continued because the dynamic response of the primary coolant in a pool-type LMR, particularly the hot pool concept, can be quite different from that in a loop-type LMR. Major modifications were made to the hot pool model, core thermal-hydraulic model,

reactivity model, and the passive decay heat-removal system model. In particular, a one-dimensional hot pool model was substituted with a more detailed two-dimensional hot pool (HP-2D) model [14], and a three-dimensional core thermal-hydraulic module was added for an accurate prediction of the temperature and velocity distributions in the core subassemblies.

Fig. 19 shows the power and flow prediction results for the UTOP accident. The UTOP is assumed to be inserted 39 cents, 2.6 cents per second for 15 seconds, by a withdrawal of all of the control rods. The power reaches a peak of 1.55 times the rated power at 42 seconds, and stabilizes at 1.09 times the rated power after 8 minutes. The net reactivity is initially positive due to the reactivity addition caused by the removal of the control rods, but turns downward once the negative reactivity feedback increases enough to counter the positive insertion. The equilibrium temperatures are reestablished after the initial phase of the UTOP, where the core remains hotter indefinitely to offset the increased reactivity, which limits the maximum reactivity insertion during the event.

The ULOF event is initiated by a trip of all primary pumps and is followed by a coastdown event. For a loss-of-flow accident, the power to the flow ratio is a key parameter that determines the consequences of the accident. The fuel temperature distribution in the hot assembly for the ULOF accident is shown in Fig. 20. The reduction of the core flow due to a pump trip causes an initial peak in the fuel centerline temperature before the power begins to fall by the effects of the reactivity feedback. It is shown that fuel damage due to a temperature increase during the initial phase of the transient is not a significant risk for this event.

The ULOHS accident is assumed to begin with a sudden loss of the normal heat sink by the IHTS and steam generators. The heat removal is achieved only by the PDRC. When the sodium heats up, the flow path of the sodium from the core to the PDRC through the hot pool is formed and the PDRC heat removal rate increases. The long-term cooling capability of the KALIMER-600 design was evaluated for different heat-removal rates through the PDRC using the SSC-K linked with a simple long-term cooling model. Fig. 21 represents the predicted pool temperatures with the PDRC heat-removal capacities. It is shown that the limit of the PDRC capacity is approximately 15.4MW. Therefore, the current PDRC design capacity of 16.5MW has a margin of nearly 1.1MW.

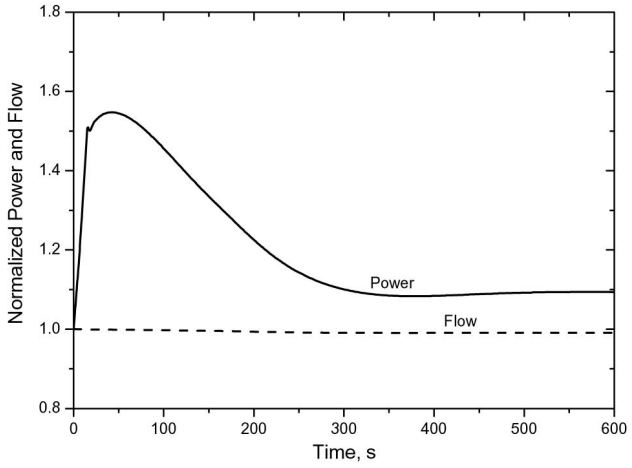

Fig. 19. Normalized Power During 30 Cents UTOP

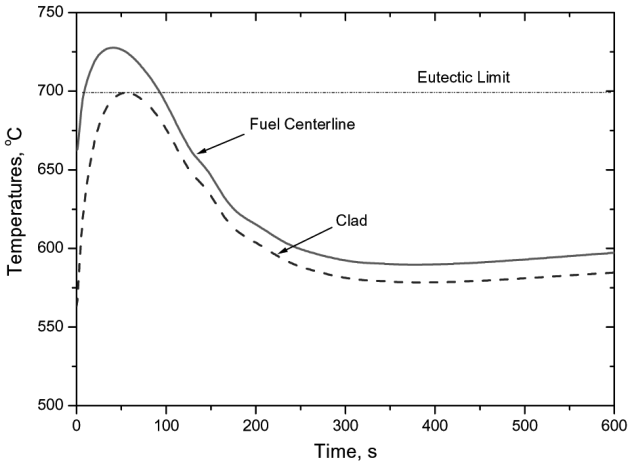

Fig. 20. Fuel Temperatures During ULOF

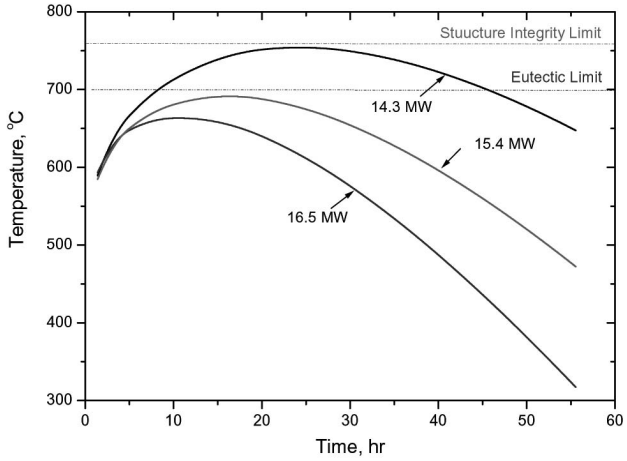

Fig. 21. Hot Pool Temperatures Predicted for Various PDRC Heat-removal Capacities

Table 4. Inherent Safety Characteristics of KALIMER-600

	DBE Limit	UTOP	ULOF	ULOHS
Peak Fuel Centerline Temp. (°C)	955	798	727	664
Peak Clad Temp. (°C)	<700	697	706	597
Peak Coolant Temp. (°C)	1055	637	694	574
Average Core Outlet Temp. (°C)	<5hr 650-700 1hr< 700-760	630	694	573

The analysis results for the different unprotected events are summarized in Table 4 and in Fig. 22, which together confirm the inherent safety characteristics of KALIMER-600. From these results, it can be said that the KALIMER-600 design accommodates various ATWS events without any threat to plant safety. The self-regulation of the power level without a scram is mainly due to the inherent and passive reactivity feedback mechanisms implemented in the design.

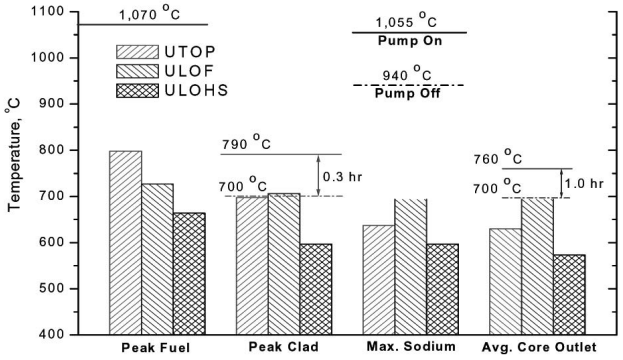

Fig. 22. Safety Limits and Margins for ATWSs

4. CONCLUSION

A conceptual design of KALIMER-600, which is an advanced sodium-cooled fast reactor rated at 600 MWe, is developed by KAERI. The design goals of sustainability, economics, safety, and proliferation resistance were implemented in the design using single enrichment fuel without blanket assemblies, passive residual heat removal, shortened intermediate heat-transport system piping and seismic isolation. The inherent safety characteristics of the developed KALIMER-600 design were verified through a safety analysis for ATWSs.

Several investigations of important thermal-hydraulic phenomena and sensing technologies were performed to support the design study. The integrity of the reactor head against creep fatigue and density-wave instability in a helical-coiled steam generator, gas entrainment on an agitating pool surface, and a sodium-water reaction were investigated. An acoustic leak detection method and a waveguide sensor visualization technology were also developed. The research and developmental efforts contribute considerably to enhance the safety, economics, and the efficiency of the KALIMER-600 design concept. KALIMER-600 is expected to serve as a reference design for the technology development of Generation IV SFR systems and in the commercialization of an SFR in Korea.

ACKNOWLEDGEMENTS

This work was performed under the Long-term Nuclear R&D Program sponsored by the Ministry of Science and Technology of the Republic of Korea.

REFERENCES

[1] H. Song, S. J. Kim, and Y. I. Kim, "Nuclear Design of A Na Cooled KALIMER-600 Core with No Blanket," Advances in Nuclear Fuel Management III (ANFM 2003), Hilton Head Island, South Carolina, USA (2003).
[2] S. G. Hong et al., "Neutronic Design of KALIMER-600 Core with Moderator Rods," Proceedings of ICAPP '04, Pittsburgh, PA, USA (2004).
[3] H. Song and Y. I. Kim, "The KALIMER-600 Core Neutronics Design with a Single Enrichment," Proceedings of GLOBAL 2005, Tsukuba, Japan, October 9-13 (2005).
[4] Eoh, J. H. et al., "Transient Performance Analysis of the Passive DHR System in KALIMER-600", Proceedings of the Korean Nuclear Society (KNS), '06 Spring Meeting, Kang-chon Resort, Korea (2006).
[5] M. R. Baum and M. E. Cook, "Gas Entrainment at the Free Surface of a Liquid: Entrainment Inception at a Vortex with an Unstable Gas Core," Nucl. Eng. Des., 32, 239-245 (1975).
[6] M. Takahashi, A. Inoue and M. Aritomi, "Gas Entrainment at Free Surface of Liquid, (I): Gas Entrain Mechanism and Rate," J. of Nuc. Sci. Tech., 25(2), 131-142 (1988).
[7] H. Madarame and T. Chiba, "Gas Entrainment Inception at the Border of a Flow-Swollen Liquid Surface," Nucl. Eng.

Des., 120, 193-201 (1990).
[8] G. Govindaraj et al., "Gas Entrainment in Surge Tank of Liquid Metal Gas Breeder Reactors," J. of Nucl. Sci. Tech., 30(7), 712-716 (1993).
[9] Y. Eguchi et al., "Gas Entrainment in the IHX Vessel of Top-entry Loop-type LMFBR," Nucl. Eng. Des., 146, 373 -381 (1994).
[10] ASME B&PV Code, Section XI, Division 3, "Rules for In-service Inspection of Nuclear Power Plant Component," ASME (1992).
[11] Y. M. Kwon, Y. B. Lee, W. P. Chang, D. Hahn, "SSC-K Code User's Manual (Rev. 0)," KAERI/TR-1619/2000, Korea Atomic Energy Research and Institute (2000).
[12] W. P. Chang et al., "Model Development for Analysis of the Korea Advanced Liquid Metal Reactor," Nucl. Eng. Des., 217, 63-80 (2002).
[13] J. G. Guppy et al., "Super System Code (SSC, Rev. 0): An Advanced Thermal Hydraulic Simulation Code for Transient in LMFBRs," NUREG/CR-3169, Brookhaven National Laboratory (1983).
[14] Y. B. Lee et al., Development of a Two-Dimensional Model for the Thermohydraulic Analysis of the Hot Pool in Liquid Metal Reactors, Annals of Nuclear Energy, 29, 21-40 (2001).